Magnetocrystalline Anisotropy of $3d^6$ and $3d^4$ Ions at Triclinic Symmetry Sites
Application to Fe^{2+} Ions in YIG: Me^{4+} (Me = Si, Ge)

Czesław Rudowicz

Institut für Physikalische und Theoretische Chemie, Universität Erlangen-Nürnberg, Erlangen*

Z. Naturforsch. **38 a**, 540–554 (1983); received August 25, 1982

The earlier suggested energy-level model based on an orbital singlet ground state for $3d^6$ and $3d^4$ ions at trigonal sites with large triclinic distortion is adopted to develop the single-ion theory of magnetic anisotropy. The Hamiltonian consisting of eight spin Hamiltonian terms and the molecular field is solved by perturbation theory. The resulting energies E_{M_S} with $M_S = 0, \pm 1, \pm 2$ are applied to calculate the free energy for Fe^{2+} ions in Si- or Ge-substituted yttrium iron garnets where a uniform distribution of Fe^{2+} ions over the 12 inequivalent sites is assumed. It turns out that the first two cubic anisotropy constants K_1 and K_2 are insufficient to describe the anisotropy at high temperatures in the present model. By a least-squares method it is established that the anisotropy expansion series can be terminated at the fourth-order term for the present model. Thus K_1, K_2, K_3 and K_4 are derived analytically in terms of the free energy for some choosen directions of magnetization. The analytical results agree very well with the corresponding ones obtained by the least-squares method. The temperature dependence of K_i, $i = 1, 2, 3,$ and 4, is calculated for a wide range of the spin Hamiltonian parameters ($B_q^{(k)}$) and the molecular field (h). The theoretical K_1 and K_2 are fitted to the experimental values of K_1 and K_2 at low temperatures obtained by neglecting the higher-order anisotropy terms, to get the values of $B_q^{(k)}$ and h for YIG:Si and YIG:Ge. A comparison of the present results with the corresponding ones of the previous doublet model, is also discussed. The theoretical account of the experimentally observed temperature dependence of the ratio K_2/K_1 for Fe^{2+} in YIG:Ge speak in favour of the present model rather than the doublet model. The change in sign of K_1 observed for Fe^{2+} in YIG:Si, which could not be explained by the doublet model with uniform distribution of Fe^{2+} ions, is well accounted for by the present model. The recently observed spin reorientation in YIG:Si can also be explained by the present model without resorting to a nonuniform distribution of Fe^{2+} ions required by the previous model. This study indicates that the higher-order constants K_3 and K_4 are significant at high temperatures according to the present model, whereas at low temperatures according to the doublet model. Hence an experimental determination of K_3 and K_4 over a wide temperature range may provide a test of the applicability of the two models.

1. Introduction

It is well recognized that the ferrous ions induced by tetravalent dopants are responsible for interesting photomagnetic effects [1–3] and magnetic circular dichroism [3–5] in substituted yttrium iron garnet (YIG). Quite recently also a spin reorientation has been observed in YIG:Si [6, 7]. The previous energy-level model for the induced Fe^{2+} ion, which was based on a ground doublet state [8], could not satisfactorily explain some of the experimental results [3].

Our earlier studies [9, 10] have provided a novel energy-level model for Fe^{2+} ions in YIG:Me^{4+}. Due to the effect of nontrigonal crystal field, which was originally suggested for Fe^{2+} in YIG:Si [11], the ground state of Fe^{2+} ion appears to be an orbital singlet. Thus by the general method [12], a triclinic symmetry spin Hamiltonian has been derived and the eight parameters $B_q^{(k)}$ have been calculated for a wide range of values of the microscopic parameters [9, 10] suitable for Fe^{2+} in YIG:Si [11].

It is the purpose of this paper to develop the single-ion theory of magnetic anisotropy [13, 14] based on the novel energy-level model [10] to study the temperature dependence of the cubic anisotropy constants. The constants K_1 and K_2 have been derived earlier explicitely at zero temperature [15].

Our preliminary calculations have indicated that the constants K_1 and K_2 are insufficient to describe

* On leave from: Solid State Division, Institute of Physics, A. Mickiewicz University, 60-769 Poznań, Poland.

Reprint requests to Dr. C. Rudowicz, Research School of Chemistry, Australian National University, P.O. Box 4, Canberra, A.C.T. 2600, Australia.

0340-4811 / 83 / 0500-0540 $ 01.3 0/0. – Please order a reprint rather than making your own copy.

the anisotropy of Fe^{2+} ion in the present model at high temperatures. The same has been found for the previous model at low temperatures. Hence a least-squares method for determination of the anisotropy constants of arbitrary order has been suggested by us [16]. It follows from this study that for the present model the anisotropy energy expansion can be terminated at the fourth-order term. Therefore we derive here analytical expressions for the cubic constants K_1, K_2, K_3 and K_4 in terms of free energy $F[hkl]$ for five choosen $[hkl]$ directions. The analytical results agree very well with the corresponding ones of the least-squares method [16]. Hence, keeping in mind the advantages of the analytical approach over the least-squares one, the former approach is mainly used in this paper.

In Sect. 2 we present a general single-ion theory of magnetic anisotropy for a singlet ground state of $3d^6$ and $3d^4$ ions at trigonal site with large triclinic distortion. The theory is applied to Fe^{2+} ion in YIG:Me^{4+} where a uniform distribution of Fe^{2+} ions over the inequivalent octahedral sites is assumed. The numerical results for energy levels, free energy and anisotropy constants, based on the earlier predicted values of the parameters $B_q^{(k)}$ [9, 10], are presented in Section 3.A. The fitting of our theory to the experimental values of K_1 and K_2 at low temperatures for Fe^{2+} in YIG:Si [17] and YIG:Ge [18] is considered in Section 3.B. A comparison with the corresponding results of the previous model is also discussed.

Based on our model the minimum of free energy of Fe^{2+} ion in YIG:Me^{4+} and the spin reorientation in YIG:Si will be studied in a subsequent paper [19].

2. Single-ion theory of magnetic anisotropy

For a $S=2$ ground singlet of $3d^6$ ($3d^4$) ion at triclinic symmetry we consider a Hamiltonian consisting of the isotropic exchange interaction in the molecular field approximation $\mathscr{H}_{mf}$ [14] and the zero-field triclinic symmetry spin Hamiltonian $\mathscr{H}_{ZF}$ [9, 10]:

$$\begin{aligned}\mathscr{H} = \mathscr{H}_{mf} + \mathscr{H}_{ZF} &= h\hat{S}_\zeta \\ &+ B_0\tilde{O}_0^{(2)} + B_1(\tilde{O}_{+1}^{(2)} - \tilde{O}_{-1}^{(2)}) + B_2(\tilde{O}_{+2}^{(2)} + \tilde{O}_{-2}^{(2)}) \\ &+ C_0\tilde{O}_0^{(4)} \quad + C_1(\tilde{O}_{+1}^{(4)} - \tilde{O}_{-1}^{(4)}) + C_2(\tilde{O}_{+2}^{(4)} + \tilde{O}_{-2}^{(4)}) \\ &+ C_3(\tilde{O}_{+3}^{(4)} - \tilde{O}_{-3}^{(4)}) + C_4(\tilde{O}_{+4}^{(4)} + \tilde{O}_{-4}^{(4)}) . \qquad (1)\end{aligned}$$

where $h = g\,\mu_B H_{ex}$ is the molecular field and the spin Hamiltonian parameters are abbreviated as $B_q^{(2)} = B_q$ and $B_q^{(4)} = C_q$ [15]. The direction ζ of magnetization $\boldsymbol{M}$ is described by the direction cosines (l, m, n) in the cubic system with the axes along the $\langle 100\rangle$-directions. We adopt the Alben's et al. [11] model of twelve orientationally inequivalent sites at distorted trigonal symmetry centers. The Hamiltonian (1) holds for each site provided the operators $\tilde{O}_q^{(k)}(\hat{S}_x, \hat{S}_y, \hat{S}_z)$ are expressed in the x, y and z local axes which differ for each site [11]. We denote by Θ_i the angle between one of the [111]-axes and the ζ-direction, whereas by φ_{ij} the ange between the local x_{ij}-axis and the projection of $\boldsymbol{M}$ on the local xy-plane.

We confine our considerations to the temperature range well below T_C where $\mathscr{H}_{mf}$ is much larger in magnitude than $\mathscr{H}_{ZF}$ and the later term can be treated as a perturbation to the former one [14, 20]. At temperatures approaching T_C the perturbation theory is no longer applicable and a simultaneous diagonalization of the total matrix $(\mathscr{H}_{mf} + \mathscr{H}_{ZF})$ would be required. However the magnetic anisotropy measurements rarely concern this temperature range [1, 14].

In order to solve the Hamiltonian (1) by perturbation theory we transform the $\mathscr{H}_{ZF}$ into a coordinate system with a z'-axis along the ζ-direction in the way used earlier [20]. The energies E_{M_S} with $M_S = 0, \pm 1$ and ± 2 are then derived including terms linear in B_q and C_q, quadratic in B_q, mixed $B_q C_q$ and cubic in B_q as follows:

$$\begin{aligned}E_0 &= E_a + E_b , \\ E_a &= (3/2)\,B_0(3p^2-1) - 3eB_1 pq \\ &\quad + (3/2)\,eB_2(2q^2+p^2-1) , \\ E_b &= (9/8)\,C_0(35p^4-30p^2+3) \\ &\quad + (9\sqrt{5/2})\,C_1(3p-7p^3)q \\ &\quad + (9\sqrt{10}/2)\,C_2[\tfrac{1}{2}(7p^4-8p^2+1) + (7p^2-1)q^2] \\ &\quad - 9\sqrt{35}\,C_3[2pq^3 + (3/2)(p^3-p)q] \\ &\quad + 9\sqrt{70}\,C_4[\tfrac{1}{8}(p^4+2p^2+1) + (p^2-1)q^2 + q^4] , \qquad (2) \\ E_{\pm 1} &= \pm h + \tfrac{1}{2}E_a - (2/3)\,E_b \\ &\quad \pm (9/4h)\,\{(3/8)\,B_0^2(23p^4-26p^2+3) \\ &\quad + B_1^2[(23p^2-8)q^2 - 8p^2 + 3] \\ &\quad + B_2^2[23q^4 + 23(p^2-1)q^2\end{aligned}$$

$$
\begin{aligned}
&+(1/4)(23p^4-14p^2+3)]\\
&-\tfrac{1}{2}eB_0B_1(23p^3-13p)q\\
&+\tfrac{1}{2}eB_0B_2[(23p^2+3)q^2+\tfrac{1}{2}(23p^4-20p^2-3)]\\
&-B_1B_2[46pq^3+(23p^3-39p)q]\}\pm 2E_c\\
&+(27/4h^2)\{(3/4)B_0^3(33p^6-49p^4+16p^2)\\
&+\tfrac{1}{2}eB_0^2B_1(-sp^5+98p^3-16p)q\\
&+eB_0^2B_2[(1/4)(sp^6-149p^4+50p^2)\\
&+\tfrac{1}{2}(sp^4-50p^2)q^2]\\
&+B_0B_1^2[2(sp^4-61p^2+4)q^2\\
&+\tfrac{1}{2}(-48p^4+31p^2)]\\
&+B_0B_2^2[\tfrac{1}{2}(sp^6-151p^4+52p^2)\\
&+2(sp^2-1)q^4+2(sp^4-100p^2+1)q^2]\\
&+B_0B_1B_2[2(-sp^5+148p^3-33p)q\\
&+4(-sp^3+25p)q^3]\\
&+eB_1^3[4(-11p^3+4p)q^3+(16p^3-5p)q]\\
&+eB_1^2B_2[4(33p^2-4)q^4\\
&+(66p^4-122p^2+13)q^2+\tfrac{1}{2}(-16p^4+21p^2)]\\
&+eB_1B_2^2[-132pq^5+(-132p^3+164p)q^3\\
&+(-33p^5+66p^3-38p)q]\\
&+eB_2^3[44q^6+66(p^2-1)q^4\\
&+(33p^4-50p^2+22)q^2\\
&+\tfrac{1}{2}(11p^6-17p^4+6p^2)]\}\,, \qquad (3)
\end{aligned}
$$

where

$$
\begin{aligned}
E_c &= (9\sqrt{15}/4h)\\
&\cdot\{(\sqrt{15}/8)B_0C_0(-21p^6+25p^4-3p^2-1)\\
&+(\sqrt{3}/2)B_0C_1(21p^5-16p^3-p)q\\
&+\tfrac{1}{2}eB_0C_2[\tfrac{1}{2}(-21p^6+31p^4-9p^2-1)\\
&+(-21p^4+10p^2+1)q^2]\\
&+(\sqrt{21}/2)B_0C_3[4(3p^3-p)q^3\\
&+3(3p^5-4p^3+p)q]\\
&+(\sqrt{42}/2)B_0C_4[2(-3p^2+1)q^4\\
&+2(-3p^4+4p^2-1)q^2\\
&+(1/4)(-3p^6+7p^4-5p^2+1)]\\
&+(\sqrt{10}/4)B_1C_0(21p^5-18p^3+5p)q\\
&+(\sqrt{2}/2)B_1C_1[(-42p^4+18p^2-2)q^2+5p^2-1]\\
&+B_1C_2[6(7p^3-p)q^3+(21p^5-24p^3-p)q]\\
&+(\sqrt{14}/2)B_1C_3[-24p^2q^4\\
&+2(-9p^4+9p^2+1)q^2+p^2-1]\\
&+(3\sqrt{7}/2)B_1C_4[8pq^5+8(p^3-p)q^3\\
&+(p^5-2p^3+p)q]\\
&+(\sqrt{10}/8)B_2C_0[2(-21p^4+18p^2-1)q^2\\
&-21p^6+39p^4-19p^2+1]\\
&+(\sqrt{2}/2)B_2C_1[6(7p^3-3p)q^3\\
&+(21p^5-30p^3+11p)q]\\
&+\tfrac{1}{2}B_2C_2[12(-7p^2+1)q^4\\
&+12(-7p^4+8p^2-1)q^2-21p^6+45p^4-21p^2+1]\\
&+(\sqrt{14}/2)B_2C_3[24pq^5+30(p^3-p)q^3\\
&+(9p^5-18p^3+7p)q]\\
&+(\sqrt{7}/2)B_2C_4[-48q^6+72(-p^2+1)q^4\\
&+2(-15p^4+30p^2-11)q^2\\
&-3p^6+9p^4-5p^2-1]\}\,,
\end{aligned}
$$

$$
\begin{aligned}
E_{\pm 2} &= \pm 2h+GB+GC\\
&\pm GBB\pm GBC+GBBB\,, \qquad (4)
\end{aligned}
$$

where we denote the contributions to facilitate the discussion in the next section, we have

$$
\begin{aligned}
&GB=-E_a\,,\quad GC=(1/6)E_b\,,\quad GBC=-E_c\,,\\
&GBB=+(9/2h)\{(3/8)B_0^2(-11p^4+10p^2+1)\\
&\quad+B_1^2[(-11p^2+2)q^2+2p^2+1]\\
&\quad-B_2^2[11q^4+11(p^2-1)q^2\\
&\quad+(1/4)(11p^4-14p^2-1)]\\
&\quad+\tfrac{1}{2}eB_0B_1(11p^3-5p)q\\
&\quad-\tfrac{1}{2}eB_0B_2[(11p^2-1)q^2+\tfrac{1}{2}(11p^4-12p^2+1)]\\
&\quad+B_1B_2[22pq^3+(11p^3-15p)q]\}\,,\\
&GBBB=-(27/4h^2)\\
&\quad\cdot\{(3/8)B_0^3(57p^6-77p^4+19p^2+1)\\
&\quad+(e/4)B_0^2B_1(-tp^5+154p^3-19p)q\\
&\quad+(e/4)B_0^2B_2[(tp^4-94p^2-1)q^2\\
&\quad+\tfrac{1}{2}(tp^6-265p^4+93p^2+1)]
\end{aligned}
$$

$$
\begin{aligned}
&+B_0B_1^2[(tp^4-92p^2+5)q^2-15p^4+5p^2+1]\\
&+B_0B_2^2[(tp^2-17)q^4+(tp^4-188p^2+17)q^2\\
&+\tfrac{1}{4}(tp^6-299p^4+125p^2-5)]\\
&+B_0B_1B_2[2(-tp^3+47p)q^3\\
&+(-tp^5+248p^3-57p)q]\\
&+2eB_1^3[(-19p^3+5p)q^3+5p^3q]\\
&+eB_1^2B_2[(114p^2-10)q^4\\
&+(57p^4-92p^2+5)q^2-5p^4+5p^2+1]\\
&+eB_1B_2^2[-114pq^5+(-114p^3+134p)q^3\\
&+(57/2)(-p^5+2p^3-p)q]\\
&+eB_2^3[38q^6+57(p^2-1)q^4\\
&+\tfrac{1}{2}(57p^4-94p^2+37)q^2\\
&+(1/4)(19p^6-37p^4+17p^2+1)]\},
\end{aligned}
$$

where above $p=\cos\Theta_i$, $q=\sin\Theta_i\cos\varphi_{ij}$, $e=\sqrt{6}$, $t=171$ and $s=99$.

We adopt here the following identification of the octahedral sites: $i=1$, the sites on the original trigonal axis [111], $i=2$, the sites on the $[1\bar{1}1]$ axis, $i=3$, the sites on the $[\bar{1}\bar{1}1]$ axis and $i=4$, the sites on the $[\bar{1}11]$ axis. Using the directions in cubic axes of the (x, y, z) local axes for each of the 12 orientationally inequivalent sites (Table II of [11]) we express the quantities p and q in (2−4) in terms of the direction cosines (l, m, n). The results are given in Table 1 below.

The averages of the angle-dependent quantities involved in (2−4) over the 12 inequivalent sites defined above are found in the form $(a+b\,\Phi+c\,Q)$, where $\Phi=l^2m^2+l^2n^2+m^2n^2$, $Q=l^2m^2n^2$ and the coefficients a, b, c are presented in Appendix 1. On averaging the lowest energy E_{-2} we have earlier derived the cubic anisotropy constants K_1 and K_2 at zero temperature [15]. We note, however, that the factor (5/24) at B_2^2 in the expression for P_1 should read (77/24). Consequently the values of K_2 in Table I therein change slightly for low values of the parameter Δ. Otherwise all conclusions in Sect. III of [15] remain valid.

The energies $E_{M_S}(\Theta_i, \varphi_{ij})$ in (2−4) enable one to compute the free energy for an arbitrary direction $[h\,k\,l]$ of magnetization for a given site '$i\,j$'. The free energy per magnetic ion is thus given by [13, 14]:

$$
\begin{aligned}
F[h\,k\,l] = &-(k\,T/12)\sum_{ij} n_{ij} \\
&\cdot \ln\left\{\sum_{M_S}\exp\left(-E_{M_S}[h\,k\,l]_{ij}/k\,T\right)\right\},
\end{aligned}
\tag{5}
$$

where n_{ij} is the occupancy of the ij-th site normalized to unity (i.e., $(1/12)\sum_{ij} n_{ij}\equiv 1$). However, because of the large number of terms involved in the energies (2−4) an explicit derivation of the temperature dependence of the anisotropy constants K_1 and K_2 (cf., e.g. [20]) is out of question for the present model.

In our preliminary calculations for Fe^{2+} in YIG: Me^{4+} we have resorted to the relations [21, 13, 14]:

$$
\begin{aligned}
K_1' &= 4\,(F[110]-F[100])\,,\\
K_2' &= 9\,(3\,F[111]+F[100]-4\,F[110])\,,
\end{aligned}
\tag{6}
$$

which are valid only if the higher-order cubic anisotropy terms can be neglected [13, 14]. On the other hand, the dependance of the anisotropy energy F_a on the angle δ that magnetization makes with the direction [100] in the plane $(01\bar{1})$ has been studied to understand the spin reorientation [6, 7]. A pronounced discrepancy has been found at high temperatures between the exact anisotropy energy: $F_a(\delta)=F(\delta)-F(\delta=0^\circ)$ calculated from (5) and

Table 1. The angular functions $p=\cos\theta_i$ and $q=\sin\theta_i\cos\varphi_{ij}$ in terms of the direction cosines (l, m, n) of magnetization for the inequivalent octahedral sites. The numbers in brackets give the site label in our notation and the Alben's et al. [11] one.

j	i	1	2	3	4
	$\sqrt{3}\,p=$	$l+m+n$	$l-m+n$	$-l-m+n$	$-l+m+n$
1	$\sqrt{6}\,q=$	(1, 1) $l+m-2n$	(4, 4) $l-m-2n$	(7,3) $-l-m-2n$	(10, 2) $-l+m-2n$
2		(2, 5) $-2l+m+n$	(5, 8) $l+2m+n$	(8, 7) $2l-m+n$	(11, 6) $-l-2m+n$
3		(3, 9) $l-2m+n$	(6, 12) $-2l-m+n$	(9, 11) $-l+2m+n$	(12, 10) $2l+m+n$

the approximated one:

$$F_a(\delta) = K_1' \Phi(\delta) + K_2' Q(\delta), \quad (7)$$

with the K_i' calculated from (6). However at low temperature a good agreement is obtained (see Fig. 2, Section 3.A.2). These considerations indicate that the higher-order anisotropy terms cannot be neglected and consequently the relations (6) are not valid for our model at high temperatures.

The expansion of the cubic anisotropy energy can be written up to the 12-th power in the direction cosines of $\boldsymbol{M}$ as [22, 16]:

$$F_a = K_1 \Phi + K_2 Q + K_3 \Phi^2 + K_4 \Phi Q + K_5 Q^2 + K_6 \Phi^3 + \ldots \quad (8)$$

In order to determine the higher-order anisotropy constants in (8) a least-square method has been suggested [16] and applied to the present model as well as to some other energy-level models. This study has revealed that the anisotropy in the present model is well accounted by the first four constants, namely K_1 to K_4. As the least-square fittings are time consuming, it seems desirable to derive analytical expressions for K_1, K_2, K_3 and K_4 in terms of $F[h\,k\,l]$. It is convenient to choose $F[100] = F(\delta = 0^\circ)$, $F[111] = F(54.74^\circ)$, $F(30^\circ)$, $F(45^\circ)$ and $F[110] = F(90^\circ)$ to establish a set of four linear equations. Solving this set we obtain:

$$\begin{aligned} K_1 &= (2048/75)\,F_1 - 64F_2 + (1134/25)\,F_3 + (4/3)\,F_4, \\ K_2 &= -(2048/15)\,F_1 + 832F_2 - (3159/5)\,F_3 - (260/3)\,F_4, \\ K_3 &= -(8192/75)\,F_1 + 256F_2 - (4536/25)\,F_3 + (32/3)\,F_4, \\ K_4 &= -(16384/25)\,F_1 + 3072F_2 - (59616/25)\,F_3 - 128F_4, \end{aligned} \quad (9)$$

where we denote

$$\begin{aligned} F_1 &= F(30^\circ) - F(0^\circ), \qquad F_2 = F(45^\circ) - F(0^\circ), \\ F_3 &= F(54.74^\circ) - F(0^\circ), \quad F_4 = F(90^\circ) - F(0^\circ). \end{aligned} \quad (10)$$

The relations (9) are valid for a general case of cubic anisotropy provided the assumption $K_i \equiv 0$ for $i \geqq 5$ holds. The K_i values, $i = 1-4$, from the least-square method [16] and those from (9) are compared in Section 3.A.2.

3. Numerical results for Fe^{2+} in YIG:Si (Ge)

The calculations are devided into two parts. Part A is based on the spin Hamiltonian parameters predicted by the microscopic theory [12] using the values of the trigonal (Δ) and nontrigonal (Γ) crystal field parameters, the spin-orbit (λ) and spin-spin (ϱ) coupling constants suitable for Fe^{2+} in YIG:Me^{4+} [10]. In Part B we find the spin Hamiltonian parameters which give a good agreement between the experimental [17, 18] and our calculated values of K_1 and K_2 at low temperatures. We include also a comparison of our results with the corresponding results of the doublet model in Part B.

A) Theoretical predictions

We denote the sets of the $B_q^{(k)}$ values with $\lambda = -80$, $\varrho = 0.18$ and with $\Gamma = 200$ (Table III of Ref. [10]) as sets no. 1 to 4 for $\Delta = 300$, 400, 500 and 600 cm^{-1}, respectively, whereas those with $\Gamma = 300$ (Table V of Ref. [10]) as sets no. 5 to 9 for $\Delta = 300$ to 700 cm^{-1}, respectively. Keeping in mind the limitations of the microscopic theory [12] the $B_q^{(k)}$ values [10] may be considered to be correct only to the order of magnitude. There are no experimental results for the $B_q^{(k)}$ parameters to compare with our theoretical predictions. Nevertheless the $B_q^{(k)}$ values [10] enable us to discuss the general properties of Fe^{2+} ion in YIG:Me^{4+}.

1) Energy-level calculations

It is of interest to consider the differences in energies between the 12 orientationally inequivalent sites in the present model. It is enough for this purpose to study the properties of the ground level E_{-2} alone because all the energies (2–4) involve the site-dependent quantities p and q in the same way, i.e. as the products $p^x q^y$ with $(x + y)$ always even. Hence the sites with a given (p, q) and those with $(-p, -q)$ have the same energy properties. Moreover for a specified direction of $\boldsymbol{M}$ the combinations of (l, m, n) in Table 1 yield identical p and q and thus E_{M_S} for several sites out of the 12 inequivalent sites.

It follows from Table 1 that for the $[h\,k\,l]$ directions considered in (6) the following sites can be grouped together as energetically equivalent ones (numbers refer to the site labels):

[100]: (a) 1, 3, 4, 5, 7, 9, 10, 11; (b) 2, 6, 8, 12,
[110]: (a) 1, 7; (b) 2, 3, 8, 9; (c) 4, 10; (d) 5, 6, 11, 12,
[111]: (a) 1, 2, 3; (b) 4, 6, 8, 9, 10, 11; (c) 5, 7, 12.

The respective energy-level calculations have been performed for all the nine $B_q^{(k)}$ sets with three values

Table 2. Site variation of the lowest two energies in the present model for the three magnetization directions with the $B_q^{(k)}$ set no 3. (upper part) and set no. 7 (lower part). E_{M_S} and h in cm^{-1}.

h	[h k l]: Site group	[100]		[110]				[111]		
		a	b	a	b	c	d	a	b	c
200	$-E_{-2}$	410.8	389.1	428.8	415.1	388.6	383.4	433.7	388.7	397.8
	$-E_{-1}$	194.4	205.7	185.4	191.6	208.8	210.3	183.6	207.9	200.2
400	$-E_{-2}$	809.0	787.4	828.1	813.3	787.7	782.4	833.5	787.6	795.6
	$-E_{-1}$	395.3	406.5	385.9	392.8	407.8	409.9	383.7	407.4	401.7
200	$-E_{-2}$	407.0	389.2	417.2	406.6	395.6	389.7	418.4	393.5	398.0
	$-E_{-1}$	196.6	205.5	191.4	196.4	203.3	205.6	190.8	204.1	200.5
400	$-E_{-2}$	806.4	788.7	817.0	805.9	795.3	789.3	818.2	793.1	797.2
	$-E_{-1}$	396.8	405.7	391.5	396.9	402.9	405.6	390.9	403.9	401.1

of h (see next subsection). In Table 2 the results for two representative $B_q^{(k)}$ sets and two values of h are collected. In order to consider the effect of the fourth-order spin Hamiltonian terms in (1) on the energy levels we calculate also the ratio of the fourth-order contribution to the energy E_{-2} (4) with respect to the corresponding second-order contribution, namely GC/GBB, both terms giving rise to K_1, and GBC/GBBB, both terms giving rise mainly to K_2. It is found that the fourth-order spin Hamiltonian terms contribute significantly to energy. For some of the site groups in Table 2 the term GBC exceeds 50% of the respective second-order contribution GBBB. Thus we conclude that the fourth-order terms in (1) cannot be neglected in the present considerations. The calculations for the remaining $B_q^{(k)}$ sets reveal that for a constant Γ the contributions to E_{-2} due to the fourth-order terms increase with Δ.

For $\boldsymbol{M}$ between the [100] and [111] direction in the plane $(01\bar{1})$ we have

$$l = \cos\delta\,, \qquad m = n = (1/\sqrt{2})\sin\delta\,. \tag{11}$$

Thus from Table 1 we find the following groups of energetically equivalent sites: (a) 1, 3, (b) 2, (c) 4, 9, (d) 5, 7, (e) 6, 8, (f) 10, 11 and (g) 12. The variation of the lowest two energy levels with the angle δ is illustrated for one $B_q^{(k)}$ set and one h value in Figure 1. A change in the site distribution over the groups of energetically equivalent sites with the angle δ is then well visualized. Figure 1 provides also information on the peaks in the ground energy, which may be useful in the ferromagnetic resonance studies at low T. The ground energy for the 'g' and 'f' site group exhibits a peak at δ about 22.5° and 42.5°, respectively. Extended calculations in the range $\delta = 0°$ to 180° indicate the corresponding peaks at about 137.5° and 157.5°, and additional peaks at 90° for the 'a', 'c' and 'd' site group. For the other $B_q^{(k)}$ sets with $h = 300\ cm^{-1}$ the position of the first two peaks varies in the range of about 15° to 25° and 40° to 50°.

The predicted differences in energies between the various groups of sites for several directions of $\boldsymbol{M}$ considered in Table 2 and Fig. 1 are not large enough to be responsible for a permanent preferen-

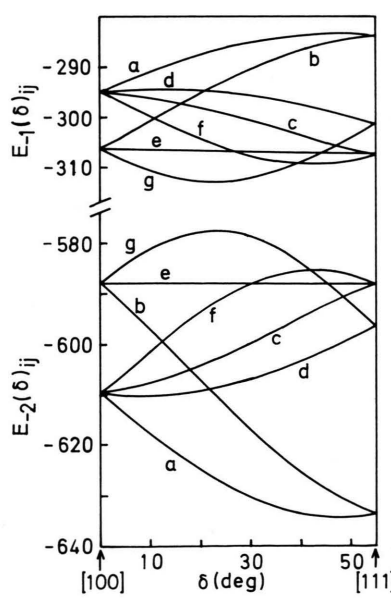

Fig. 1. The variation of the lowest two energies with the angle δ for the seven groups of energetically equivalent sites 'a' to 'g' (see text) with the $B_q^{(k)}$ set no. 3 and $h = 300\ cm^{-1}$. Note the discontinuity in the ordinate.

tial occupation of the Fe^{2+} sites in YIG:Me^{4+} in a wide temperature range. The magnitude of the differences in energies suggests that they can account for specific preferential site occupancies only at very low temperatures.

2) Free energy and anisotropy constants

Basing on the above results we consider in this paper only the uniform distributions of the Fe^{2+} ions over the 12 inequivalent sites. Thus we put $n_{ij} \equiv 1$ in (5) for all ij. No intrinsic variation of the molecular field h with temperature is taken into account. In the temperature range 0–300 K the molecular field in pure YIG can be regarded as nearly constant [14, 23]. However, for a general discussion of the effect of h on the properties of Fe^{2+} ion in the present model, we have performed the calculations for several values of h, namely, 200, 300 and 400 cm^{-1}, being close to the values reported for substituted YIG [11, 14, 24, 25].

The final program computes the following quantities as a function of temperature for each $(B_q^{(k)}, h)$ set:

(i) the free energy $F[110]$ and $F(\delta)$ with δ varying in steps 5° between 0° and 50° and with the last $\delta = 54.74°$ from (5) and then the anisotropy energy:

$$F_a^t(\delta_q) = F(\delta_q) - F(\delta = 0°), \tag{12}$$

(ii) the K_1' and K_2' from (6),

(iii) the K_i from (9) and the ratio $|K_i/K_1|$ for all i,

(iv) the K_{1a} and K_{2a} by the least-square fitting [16] of the 'approximated' anisotropy energy curve (8) with $K_i \equiv 0$ for $i \geqq 3$ to the exact 'points' (12).

In general we denote the K_i values fitted by the method [16] as $K_{i\varepsilon}$ with $\varepsilon = a$ to d for a fitting with the first 2, 3, 4 and 5 terms of (8) taken into account, respectively. The results of these fittings are compared with the approximate analytical ones from (6) and (9) in Table 3 for one choosen $(B_q^{(k)}, h)$ set. The discrepancy between the points $F_a^t(\delta_q)$ calculated from (12) and the curve $F_a(\delta)$ based on (7), mentioned in Sect. 2, is illustrated for this case in Figure 2. The corresponding curves based on (8) with the K_i as well as these with the K_{ic} from Table 3 ($K_5 = K_6 = 0$) pass exactly through the points for all temperatures. For clarity of the graph we omit these curves from Figure 2. The goodness of a fit is well accounted by the standard deviation σ [16] of the exact and approximate curve. The importance of a given term $K_{i\varepsilon} f_i(\delta)$ in the expansion

Table 3. The present model anisotropy constants (in cm^{-1}/Fe^{2+} ion) calculated by various procedures (see text) with the $B_q^{(k)}$ set no. 6 and $h = 300$ cm^{-1}.

T	10	100	150	225	300
K_1	−0.0138	−0.0089	−0.0041	−0.0019	−0.0020
K_{1a}	−0.0138	−0.0099	−0.0058	−0.0037	−0.0036
K_2	−0.0857	−0.0672	−0.0403	−0.0151	−0.0053
K_{2a}	−0.0857(69)	−0.0586(66)	−0.0246(47)	+0.0022(6)	+0.0095(30)
σ^2	7.5 *E*-16	1.3 *E*-10	3.6 *E*-10	3.5 *E*-10	2.3 *E*-10
K_{1b}	−0.0138	−0.0103	−0.0065	−0.0044	−0.0041
K_{2b}	−0.0857(69)	−0.0802(87)	−0.0601(103)	−0.0330(84)	−0.0189(51)
K_{3b}	0.0000(0)	0.0083(27)	0.0137(70)	0.0135(103)	0.0109(89)
σ^2	1.7 *E*-16	1.3 *E*-12	2.5 *E*-12	1.6 *E*-12	7.3 *E*-13
K_{1c}	−0.0138	−0.0103	−0.066	−0.045	−0.041
K_{2c}	−0.0859(69)	−0.0640(69)	−0.0381(64)	−0.0156(39)	−0.0070(19)
K_{3c}	0.0000(0)	0.0051(16)	0.0093(47)	0.0101(75)	0.0086(69)
K_{4c}	+0.0002(0)	−0.0178(6)	−0.0243(14)	−0.0191(16)	−0.0131(12)
σ^2	6.1 *E*-17	1.9 *E*-15	1.9 *E*-15	5.8 *E*-16	1.8 *E*-16
K_1	−0.0138	−0.0103	−0.0065	−0.0044	−0.0041
K_2	−0.0856	−0.0664	−0.0407	−0.0172	−0.0079
K_3	0.0000	0.0054	0.0097	0.0103	0.0087
K_4	−0.0003	−0.0144	−0.0206	−0.0169	−0.0118
K_{1d}	−0.0138	−0.0103	−0.0066	−0.0045	−0.0045
K_{2d}	−0.0862(69)	−0.0661(71)	−0.0401(68)	−0.0168(42)	−0.0076(20)
K_{3d}	0.0001(0)	0.0057(18)	0.0099(50)	0.0104(78)	0.0087(70)
K_{4d}	0.0001(0)	−0.0182(7)	−0.0247(14)	−0.0194(16)	−0.0132(12)
K_{5d}	0.0019(0)	0.0134(1)	0.0132(1)	0.0074(1)	0.0041(0)
σ^2	2.3 *E*-17	9.8 *E*-18	2.7 *E*-18	2.1 *E*-19	6.6 *E*-20

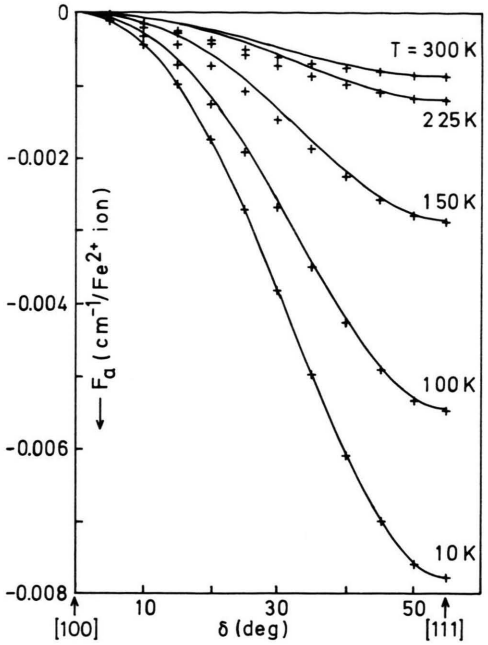

Fig. 2. The theoretical anisotropy energy F_a vs. the angle δ with the $B_q^{(k)}$ set no. 6 and $h = 300\ cm^{-1}$. The points represent the exactly calculated values, whereas the full lines represent the 'second-rank' approximate curve.

(8), where $f_i(\delta)$ is the respective angle-dependent function, can be accounted by the percentage ratio of $|K_{i\varepsilon} f_i(\delta)|$ with respect to $|K_{1\varepsilon} f_1(\delta)|$ [16]. This ratio attains the maximum value for $\delta = 54.74°$, where the functions $f_i(\delta)$ have maximum [16], and this value is given in brackets in Table 3 (zero means a value less than 0.5%).

The drawings in Fig. 2 and a comparison of K_i' with K_{ia}, $i = 1$ and 2, in Table 3 reveal an inadequacy of the approximation made in (6) and hence the importance of the higher-order anisotropy terms. If this approximation is good one excepts $K_1' = K_{1a}$ and $K_2' = K_{2a}$, but the actual calculations show that this is not true for several $(B_q^{(k)}, h)$ sets at high temperatures. From Table 3 it is evident that a termination of the series in (8) at the fourth-order term and the use of the approximate relations (9) for the $B_q^{(k)}$ set no. 6 is well justified. This conclusion can be safetly extended for the remaining $B_q^{(k)}$ sets for which the discrepancy between K_i' and K_{ia}, $i = 1$ and 2, is comparable or less pronounced than for the $B_q^{(k)}$ set no. 6. Thus the other results presented below are based on the analytical relations (9).

We adopt the criterion [26] that the maximum value of a given term $|K_i f_i(\delta)|$ should be greater than 10% of $K_1 f_1(\delta)$ in order to consider the term as significant. Thus for the direction [111] this criterion means that the ratio $|K_i/K_1|$ should be greater than 0.90, 0.30 and 2.70 for $i = 2$, 3 and 4, respectively. In Table 4 we list the temperature ranges for which the above criterion is satisfied. It is seen in Table 4 that the higher-order anisotropy terms are the most important for the $B_q^{(k)}$ set no. 1 and 6. The temperature dependance of the K_i's for the two sets is illustrated in Figure 3. For comparison the corresponding $K_i'(T)$ from (6) with $h = 200\ cm^{-1}$ are also plotted in Figure 3. The discrepancy between K_i' and K_i, $i = 1$ and 2, is then well visualized.

The behaviour of $K_i(T)$ for the other $B_q^{(k)}$ sets is to great extend similar to that with the $B_q^{(k)}$ set no. 1 (Figure 3a). Hence, instead of graphical presentation, we tabulate the salient features of $K_1(T)$ and $K_2(T)$ in Table 5, whereas $K_3(T)$ and $K_4(T)$ in Table 6. These Tables give an idea about the predicted range of values attained by the anisotropy constants K_i, $i = 1-4$, for Fe^{2+} ion in YIG:Me^{4+} in the temperature range 0–300 K. The variation of $K_i(T)$ with the crystal field parameter Δ for two values of Γ considered is also illustrated by Table 5 and 6. We note that for $\Gamma = 300\ cm^{-1}$ the sign of K_1 changes between the set no. 6 ($\Delta = 400$) and 7

Table 4. The temperature ranges t_i (in °K) where the anisotropy terms $K_i f_i$ are important with respect to the first term $K_1 f_1$ in the present model[a].

$B_q^{(k)}$ set	h[c]	t_2	t_3	t_4
1	200	0–105, 230–260	70–300	110–300
	300	0–100	170–300	–
2[b]	200	0–90, 285–300	210–300	265–300
3	200	0–130, 285–300	–	–
	300	0–110	–	–
4	200	0–200, 230–300	275–300	–
	300	0–160	–	–
5[b]	200	–	290–300	–
6	200	0–230	50–300	60–280
	300	0–300	90–300	140–300
	400	0–300	130–300	–
7[b]	200	0–75, 280–300	190–300	280–300
8[b]	200	0–75, 290–300	260–300	–
9[b]	200	0–100, 290–300	–	–

[a] A bar means the term $K_i f_i(\delta)$ is less than 10% of $K_1 f_1(\delta)$ at $\delta = 54.74°$ in the temperature range 0–300 K.
[b] With $h = 300\ cm^{-1}$ all the higher-order terms are negligible for this set.
[c] With $h = 400\ cm^{-1}$ the higher-order terms are negligible for all $B_q^{(k)}$ sets, except for the set no. 6.

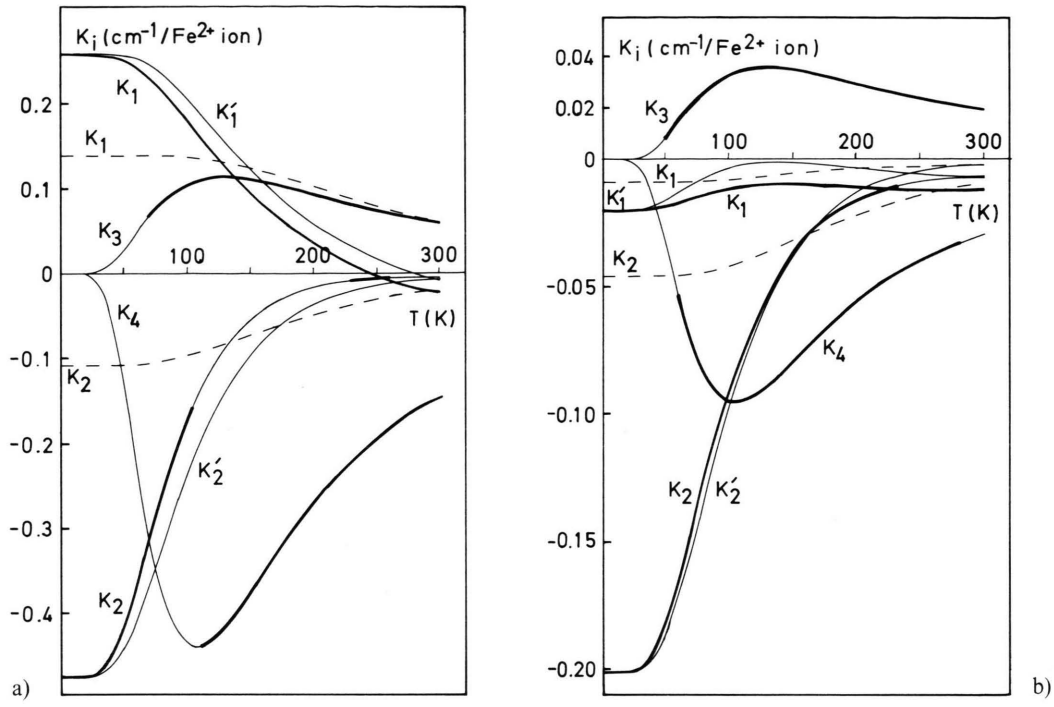

Fig. 3. The anisotropy constants vs. temperature with $h = 200$ (solid line) and 400 cm^{-1} (dashed line). The K_3 and K_4 with $h = 400$ attain to small values to be shown. A heavy line corresponds to the temperature range for which a given term is important with respect to the first term (see Table 4). a) The $B_q^{(k)}$ set no. 1. b) The $B_q^{(k)}$ set no. 6.

($\Delta = 500$) and that of K_2 between the set no. 5 ($\Delta = 300$) and 6 ($\Delta = 400\ cm^{-1}$). The calculations of free energy as a function of T and δ reveal that for the $B_q^{(k)}$ set no. 5 and 6 the minimum of $F(\delta)$ is in the direction [111], whereas for the sets no. 7 to 9 in the direction [100], at all T and for all h considered. Another interesting feature is a gradual shift of the minimum of $F(\delta)$ for the $B_q^{(k)}$ set no. 1 between about 245 K and 300 K from the direction [100] to [111] with $h = 200\ cm^{-1}$, whereas with $h = 300$ and 400 cm^{-1} the minimum of $F(\delta)$ keeps in the direction [100] at all T. These results suggest that the present model with uniform distribution of Fe^{2+} ions can account for the broad spin reorientation

Table 5. The anisotropy constants K_1 and K_2 (in cm^{-1}/Fe^{2+} ion) predicted by the present model at $T = 10$ K (upper line) and $T = 300$ K (lower line).

h	$B_q^{(k)}$ set:	1	2	3	4	5	6	7	8	9
200	K_1	0.258	2.12	4.62	7.77	−0.485	−0.021	0.662	1.61	2.82
		−0.023[a]	0.037	0.148	0.341	−0.022	−0.012	0.006	0.035	0.079
	K_2	−0.475	−2.65	−6.88	−13.8	0.091	−0.201	−0.716	−1.83	−3.56
		−0.005	−0.041	−0.172	− 0.573	−0.0007[b]	−0.007	−0.014	−0.033	−0.073
300	K_1	0.177	1.41	3.05	5.10	−0.324	−0.014	0.441	1.07	1.85
		0.034	0.291	0.644	1.10	−0.067	−0.004	0.090	0.219	0.385
	K_2	−0.201	−1.21	−3.19	− 6.42	0.046	−0.086	−0.321	−0.833	−1.63
		−0.014	−0.089	−0.261	− 0.607	0.002	−0.008	−0.024	−0.062	−0.125
400	K_1	0.139	1.08	2.31	3.85	−0.244	−0.0092	0.335	0.805	1.40
		0.059	0.434	0.933	1.56	−0.095	−0.0023	0.135	0.322	0.559
	K_2	−0.107	−0.702	−1.87	− 3.79	0.029	−0.046	−0.182	−0.479	−0.943
		−0.020	−0.134	−0.372	− 0.797	0.005	−0.0094	−0.035	−0.092	−0.183

[a] K_1 changes sign at $T \approx 245$ K; [b] K_2 changes sign at $T \approx 270$ K.

observed in YIG:Si [6, 7]. This problem will be studied in detail in a subsequent paper [19].

The explicitely derived values of K_1 at 0 K [15] coincide with the corresponding ones at 10 K in Table 5. The same holds for the corrected K_2 values (see Section 2 above) of [15] and those at 10 K in Table 5.

In order to discuss the effect of the fourth-order spin Hamiltonian parameters (C_q) on the magnetic anisotropy we calculate the constants $\bar{K}_i(T)$ with the $B_q^{(k)}$ set no. 3 and 7 putting all $C_q \equiv 0$. Then the quantities $R_i(T) = |\bar{K}_i(T) - K_i(T)|/|\bar{K}_i(T)|$, where $K_i(T)$ are the corresponding constants with the full $B_q^{(k)}$ set, are calculated. For the both sets $\bar{K}_i$ is lower than K_i for $i = 1-4$. With the set no. 3 $R_1(R_2)$ shows a systematic variation in the temperature range 10 K to 300 K between (in per cent) 7–28 (9–27), 10–13 (14–23) and 14–16 (19–23) with $H = 200$, 300 and 400 cm^{-1}, respectively. Depending on the value of h, the maxima of $R_3(R_4)$ fall at different temperatures and are equal to 15 (42), 21 (58) and 25 (1200) with $h = 200$, 300 and 400, respectively. With the set no. 7 only R_1 shows a systematic variation with T and is in the range 5–82, 8–11 and 11–13 (%) with $h = 200$, 300 and 400, respectively. The maxima of R_2, R_3 and R_4 fall at different T and are as follows: for R_2–4, 2 and 3, for R_3–8, 12 and 17, for R_4–19, 26 and 35 with $h = 200$, 300 and 400, respectively. Thus we conclude that the fourth-order spin Hamiltonian terms contribute significantly to the anisotropy constants, especially to K_3 and K_4.

Table 6. The anisotropy constants K_3 and K_4 (in cm^{-1}/Fe^{2+} ion) predicted by the present model at $T = T_e$ where K_3 and K_4 has the extreme value and at $T = 300$ K ($h = 200$ cm^{-1}) [a].

$B_q^{(k)}$ set	$K_3(T_e)$	$K_3(300)$	$K_4(T_e)$	$K_4(300)$
1	0.114 (125)	0.061	−0.438 (110)	−0.145
2	0.147 (125)	0.075	−0.701 (110)	−0.245
3	0.0687(100)	0.0206	−0.535 (110)	−0.199
4	−0.233 (150)	−0.154	+0.816 (110)	+0.289
5	0.126 (130)	0.0068	−0.0388(100)	−0.0112
6	0.0359(125)	0.0196	−0.0954(100)	−0.0297
7	0.0514(130)	0.0275	−0.164 (110)	−0.0531
8	0.0574(120)	0.0298	−0.205 (110)	−0.0687
9	0.0373(110)	0.0157	−0.178 (110)	−0.0622

[a] For $h = 300$ and 400 cm^{-1} K_3 and K_4 are in general insignificant (see Table 4).

B) Comparison of the present model with experiments and with the doublet model

1) Fe^{2+} in YIG:Ge

The ferromagnetic resonance studies [18] have provided the first two anisotropy constants for YIG:Ge with several concentrations of Fe^{2+} ions in a wide temperature range. Thus the Fe^{2+} ion contributions to the anisotropy were extracted, but only at few temperatures, as follows: +4.2 and −13 at 4.2 K, +2.3 and −4.1 at 77 K, and +0.1 and −0.1 at 295 K, for K_1 and K_2 (in cm^{-1}/Fe^{2+} ion), respectively. Although explicit dependance of K_1 and K_2 on T was not presented, but the dependance of K_2/K_1 on T was explained well by the doublet model with the parameter $a = 0.42$ and $\lambda = -54$ cm^{-1} [18]. As pointed out in [10] this value of λ implies too strong covalency reduction then expected for Fe^{2+} in crystals [27], suggesting an inadequacy of the doublet model.

For comparison with our results presented in Table 5 (based on a more reasonable value of $\lambda = -80$ cm^{-1} [10]), we have computed the necessary free energies from (5) and then the K_i' (6), K_i (9) and the K_{ic} fitted by the method [16] for the doublet model with the above values of a and λ [18]. Some of the results are collected in Table 7. From these calculations it turns out that at temperatures below 40 K the fifth-rank fit ($p = 5$) is not reliable for this case because of the opposite sign of K_{2d} and K_{3d} with respect to the fits with $p = 4$ and 3. The same is encountered [16] for the doublet model with $a = 0.5$ [24], while it is not observed for $a = 0.853$ [28]. Therefore in the discussion below we rely on the analytical K_i's which agree well with the fitted K_{ic}'s. As it is seen from Table 7 the doublet model predicts the significance of K_3 and K_4 at low temperatures, whereas the present model at high temperatures (see Table 4). Hence, an experimental determination of the K_3 and K_4 in a wide temperature range may provide an useful test of applicability of the two models.

If the higher-order anisotropy terms are taken into account in the analysis of the experimental data [18] one expects somewhat different values of K_1 and K_2 then those quoted above. Nevertheless the theoretical K_i values ($i = 1, 2$) in Table 2 are several times higher then the corresponding experimental ones [18]. On contrary, the K_i values with the set no. 3 and 4 in Table 5 are quite close to the experi-

Table 7. The doublet model anisotropy constants (in cm^{-1}/Fe^{2+} ion) calculated by various procedures (see Sect. 3.A.2) with $a = 0.42$ and $\lambda = -54\ cm^{-1}$.

T	10	50	100	150	200	300
K_1	19.38	15.86	6.943	3.019	1.492	0.5000
K_{1a}	18.28	15.24	6.853	3.005	1.489	0.4998
K_2	− 55.89	−38.09	− 9.650	−2.490	−0.7872	−0.1302
K_{2a}	− 44.75(27)	−31.94(23)	− 8.793(14)	−2.363(8)	−0.7620(6)	−0.1282(3)
σ^2	2.0 *E*-03	3.7 *E*-04	2.8 *E*-06	3.2 *E*-08	8.5 *E*-10	1.1 *E*-10
K_{1b}	16.73	14.56	6.794	2.999	1.488	0.4997
K_{2b}	−126.2(84)	−67.33(51)	−11.88(19)	−2.697(10)	−0.8164(6)	−0.1318(3)
K_{3b}	31.28(62)	13.60(31)	1.187(6)	0.1282(1)	0.0209(0)	0.0014(0)
σ^2	5.5 *E*-05	9.6 *E*-06	4.8 *E*-08	3.1 *E*-10	4.4 *E*-12	6.5 *E*-15
K_{1c}	16.31	14.38	6.781	2.998	1.488	0.4997
K_{2c}	− 25.37(17)	−24.34(19)	− 8.845(14)	−2.454(9)	−0.7872(6)	−0.1307(3)
K_{3c}	11.37(23)	5.105(12)	0.5874(3)	0.0801(1)	0.0151(0)	0.0012(0)
K_{4c}	−111.0(25)	−47.36(12)	− 3.346(2)	−0.2680(0)	−0.0322(0)	−0.0012(0)
σ^2	3.0 *E*-06	7.5 *E*-08	2.4 *E*-12	2.0 *E*-14	2.4 *E*-16	2.1 *E*-18
K_1	16.60	14.48	6.786	2.998	1.488	0.4997
K_2	− 33.18	−29.08	− 9.159	−2.472	−0.7886	−0.1307
K_3	11.11	5.503	0.6260	0.0824	0.0153	0.0012
K_4	− 93.13	−39.39	− 2.882	−0.2422	−0.0301	−0.0012
K_{1d}	16.45	14.40	6.781	2.998	1.488	0.4997
K_{2d}	+ 54.58(37)	−11.92(9)	− 8.820(14)	−2.460(9)	−0.7880(6)	−0.1307(3)
K_{3d}	− 11.31(23)	+ 1.582(4)	0.5804(3)	0.0821(1)	0.0154(0)	0.0012(0)
K_{4d}	− 94.29(21)	−44.76(12)	− 3.341(2)	−0.2695(0)	−0.0324(0)	−0.0012(0)
K_{5d}	−504.2(13)	−78.29(2)	− 0.1555(0)	+0.0437(0)	+0.0052(0)	+0.0004(0)
σ^2	2.7 *E*-07	1.0 *E*-08	2.2 *E*-12	1.0 *E*-15	5.3 *E*-18	1.6 *E*-18

mental ones, however the ratio K_2/K_1 vs. T does not follow exactly the experimentally observed one. Thus it is of interest to find out whether our theoretical K_1 and K_2 with some other $B_q^{(k)}$ and h values could be fitted to the experimental data [18] on K_1, K_2 and K_2/K_1 at the same time. So the explicitely derived K_1 and K_2 at 0 K [15] are fitted to the experimental values at 4.2 K (see above) by varying h, B_0, B_1, B_2, C_0 and C_1 in small steps, while keeping C_2, C_3 and C_4 constant. In this process one ends up with several $(B_q^{(k)}, h)$ sets from which the sets with B_q and C_q closest to the earlier predicted ones [10] are choosen. Then the program described in Sect. 3.A.2 is run with these $(B_q^{(k)}, h)$ sets to get the temperature dependance of the K_i's. The $(B_q^{(k)}, h)$ sets which yield K_2/K_1 vs. T best matching with the experimentally observed K_2/K_1 [18], are now choosen.

A striking result of these calculations is that in a range of $h \approx 260$ to $275\ cm^{-1}$ it is possible to find suitable $B_q^{(k)}$ sets which yield K_2'/K_1' increasing smoothly with T, whereas K_2/K_1 bends at a certain T. This situation is illustrated in Fig. 4 with $h = 275$, $B_0 = 14.4$, $B_1 = -4.5$, $B_2 = -4.5$, $C_0 = 0.230$, $C_0 = -0.110$, and with $C_2 = 0.0035$, $C_3 = -0.0002$ and $C_4 = 0.0004$ (cm^{-1}). Similar results are obtained with $h = 265$, $B_0 = 14.6$, $B_1 = -5.0$, $B_2 = -4.2$, $C_0 = 0.220$, $C_1 = -0.090$ and with C_2, C_3 and C_4 as above. For both the $(B_q^{(k)}, h)$ sets K_3 is important at T above 125 K, while K_4 is important only for the second set above 260 K. The above B_2 values, although higher than the ones predicted for Fe^{2+} in YIG:Me^{4+} [10], are close to the B_2 values for Fe^{2+} in other compounds [29]. In view of the large B_0 values, the fitted B_2 values are also quite reasonable.

Figure 4 reveals a discrepancy between the curve $r_d = K_2/K_1$ and $r_d' = K_2'/K_1'$ for the doublet model at low T. The curve r_d' matches well the experimental points K_2'/K_1' for Fe^{2+} in three samples of YIG:Ge (see Fig. 5 of [18]) which appear to be scattered mostly above the curve r_d' at low T and below r_d' at high T. The experimental points K_2'/K_1' were obtained by neglecting the higher-order anisotropy terms in the analysis of the resonance data [18]. Thus a better procedure to check the applicability of the doublet model would be to fit the curve r_d to the experimental points when the constants K_3 and K_4 are taken into account in the analysis of the experimental data. On the other hand, the curve $r_p' = K_2'/K_1'$ for the present model matches reasonably

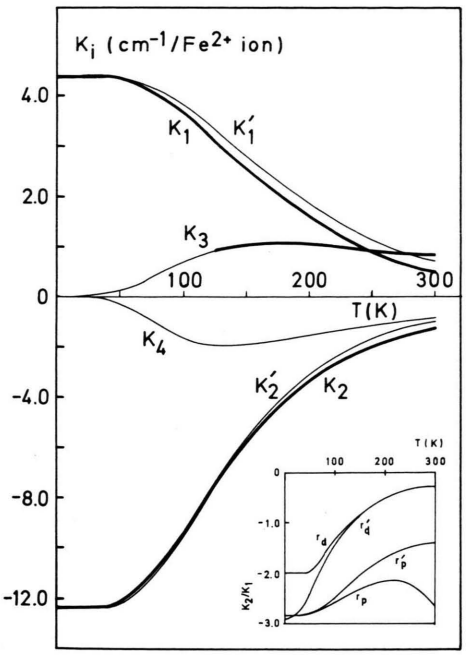

Fig. 4. The anisotropy constants vs. T with the fitted $B_q^{(k)}$ and h values (see text) for Fe^{2+} in YIG:Ge. Note the different scale for positive and negative K-axis. The inset shows the ratio of the first two constants $r = K_2/K_1$ from (9) and $r' = K_2'/K_1'$ from (6) for the present case 'p' and for the doublet model 'd' (see Table 7).

well with the existing experimental points K_2'/K_1', whereas the corresponding curve r_p exhibits a bend. These findings indicate clearly that we should not rely on the theory as well as on the interpretation of experimental data, which takes into account only the first two anisotropy constants.

It is worthwhile to mention also the results of fittings in the range of h below and above the values 260–275 cm^{-1} discussed above. A good agreement between our K_1 and K_2 and the experimental K_1' and K_2' at low T [18] can also be achieved with $h = 155$, $B_0 = 10.5$, $B_1 = -3.4$, $B_2 = -2.7$, $C_0 = 0.110$, $C_1 = -0.040$, and with $C_2 = 0.0036$, $C_3 = 0.0001$ and $C_4 = 0.0005$ (cm^{-1}). However K_1 changes sign at about 220 K and hence a discontinuity in K_2/K_1 arises. An interesting feature is a gradual shift of the minimum of free energy from the direction [100] to [111] between 220 K and 275 K [19]. With the values of h above 300 cm^{-1} the required agreement is possible with the values of B_0 around 20 cm^{-1} which are somewhat higher than the B_0 values for Fe^{2+} in other compounds [20, 29]. Then both K_2'/K_1' and K_2/K_1 increase smoothly with T without showing a bend. One may expect that with higher values of the parameters C_q than assumed here a better agreement can be achieved even with lower values of B_0. It is worthwhile to mention that the microscopic theory [12] rather underestimates the fourth-order spin Hamiltonian parameters as compared with the experimental values (cf. the pertinent references in [20]). In view of the lack of adequate experimental data on the K_i's, we have not attempted such fits.

The above results show that the present model can account very well for the experimental K_1 and K_2 at T close to 0 K for Fe^{2+} in YIG:Ge with the values of the model parameters $B_q^{(k)}$ matching well with the earlier predicted ones [10]. But the explanation of the temperature dependance of K_2/K_1 at room temperatures requires somewhat greater values of these parameters. In view of the significant role of the constants K_3 and K_4 found both for the present model as for the doublet model, a reconsideration of the experimental data [18] taking into account the higher-order anisotropy terms is highly desirable. Then, with more reliable experimental data on the temperature dependance of K_1, K_2, K_3 and K_4, it will be worthwhile to attempt fittings in the least-square sense. This may give more adequate ($B_q^{(k)}$, h) values than those found above.

2) Fe^{2+} in YIG:Si

The torque measurements [17] have provided K_1 for YIG($Si_{0.1}$) in the temperature range 4–300 K. The striking feature was an observed change in sign of the Fe^{2+} contribution to the total K_1 from positive at very low T to negative at higher T. The explicit values of K_1 and K_2 for Fe^{2+} ion were reported only at 4 K as + 0.6 and − 1.8 (cm^{-1}/Fe^{2+} ion), respectively. The change in sign of K_1 for Fe^{2+} at low T has also been reported for YIG(Si_x) from torque measurements ($x = 0.05$ and 0.14) [30] and from ferromagnetic resonance studies ($x = 0.05$) [31]. Based on the results [31] the value $K_1 = 1.4$ and $K_2 = -2.5$ (cm^{-1}/Fe^{2+} ion) has been derived at 77 K [14, 18].

Our calculations [16] for the doublet model with the values of a and λ suitable for Fe^{2+} in YIG:Si [28, 18] indicate a large discrepancy with the experimental data on K_1 and K_2, especially with $a = 0.5$ and $|\lambda| = 71$ cm^{-1} [18]. It follows from these calcu-

lations that the observed change in sign of K_1 for Fe^{2+} in YIG:Si cannot be accounted by the doublet model with uniform distribution of Fe^{2+} ions.

On the other hand, K_1 and K_2 based on our model with $h = 150$, $B_0 = 5.9$, $B_1 = -2.5$, $B_2 = -1.7$, $C_0 = 0.016$, $C_1 = -0.017$ and with $C_2 = 0.0015$, $C_3 = 0.0$ and $C_4 = 0.0003$ (cm^{-1}) can be fitted exactly to the experimental K_1 and K_2 at 4 K [17]. The above B_q and C_q values are very close to the ones predicted earlier [10]. These results are illustrated in Figure 5. It is seen in Fig. 5 that K_3 and K_4 play an important role in a wide temperature range. These $B_q^{(k)}$ and h values yield a change in sign of K_1' at about 225 K, while of K_1 at about 195 K. The latter temperature is of the same order of magnitude as expected for Fe^{2+} in YIG(Si_x) with $x = 0.05$ and 0.14 [30], whereas much higher than the experimentally observed for YIG($Si_{0.1}$) [17]. The minimum of our theoretical free energy shows a gradual shift between 175 K and 250 K from the direction [100] to [111] (see [19]).

The above fit is not unique. An agreement is also achieved with, e.g. $h = 260$, $B_0 = 7.5$, $B_1 = -2.8$, $B_2 = -2.8$, $C_0 = 0.030$, $C_1 = -0.019$ and with $C_2 = 0.0016$, $C_3 = 0.0$ and $C_4 = 0.0002$ (cm^{-1}). Then $K_1 = 0.59$, $K_2 = -1.77$ at 10 K and $K_1 = 0.042$, $K_2 = -0.116$ (cm^{-1}/Fe^{2+} ion) at 300 K. However, similar to Fe^{2+} in YIG:Ge, with the above ($B_q^{(k)}$, h) values for the present system K_2/K_1 exhibits a bend at about 260 K, while K_2'/K_1' increases smoothly from -3.0 at 10 K to -1.0 at 300 K.

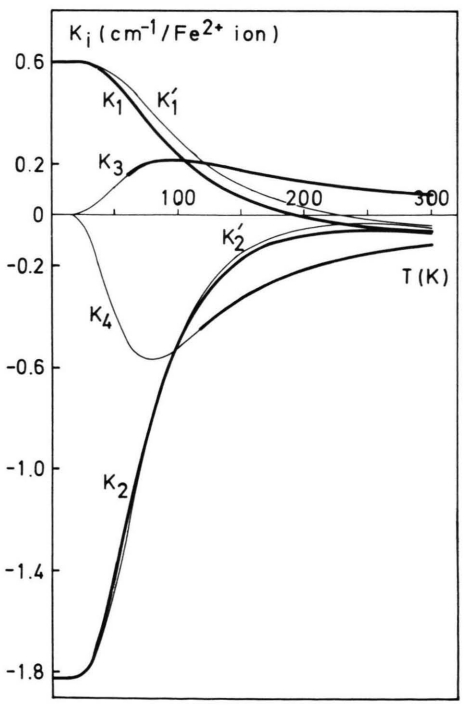

Fig. 5. The anisotropy constants vs. T with the fitted $B_q^{(k)}$ and h values (see text) for Fe^{2+} in YIG:Si.

To close this Section let us mention the difficulties in experimental determination of the actual content (z) of Fe^{2+} ions which differs from the content of Me^{4+} ions [11, 32, 7]. This aspect has not been realized in earlier anisotropy studies [17, 30, 31]. Because K_1 and K_2 for Fe^{2+} ions are not directly measurable quantities and can only be extracted from the bulk data on YIG:Me^{4+}, the value of z strongly influences the experimental values of K_1 and K_2 for Fe^{2+} ion. Hence all the above quoted experimental values of K_1 and K_2 should be treated with caution. Moreover, in all the studies [17, 18, 30, 31] the higher-order anisotropy terms have been neglected. Thus the theoretically fitted parameters $B_q^{(k)}$ and h for the present model are also subject to these uncertainties.

4. Summary

The novel energy-level model worked out earlier [9, 10] for Fe^{2+} in YIG:Si has enabled us to develop in this paper a single-ion theory of magnetic anisotropy suitable for $3d^6$ and $3d^4$ ions at trigonal sites with large triclinic distortion. This theory is applied to Fe^{2+} ions in YIG:Me^{4+} (Me = Si, Ge) assuming a uniform distribution of Fe^{2+} ions over the 12 inequivalent octahedral sites. The preliminary calculations have indicated a pronounced discrepancy between the exactly calculated anisotropy energy and the one obtained using only the cubic constants K_1 and K_2 calculated from the second-rank approximate expressions. This evidence of the importance of the higher-order anisotropy terms has led us to suggest a least-squares method to determine these terms [16]. By this method it has been established that in addition to K_1 and K_2 also the constants K_3 and K_4 should be taken into account for the present model at high temperatures and for the previous doublet model at low temperatures. Analytical expressions have been derived for K_1, K_2, K_3 and K_4 in terms of free energy for some five choosen directions of magnetization. The analytical results for K_i, $i = 1-4$, agree very well with the cor-

responding results of the least-squares method for some representative sets of the model parameters. It is also found that K_1' and K_2' obtained by neglecting the higher-order anisotropy terms differ significantly from K_1 and K_2 (obtained along with K_3 and K_4) in a wide temperature range. The analytical approach is used to study the temperature dependance of the K_i's, $i = 1-4$, for a wide range of the spin Hamiltonian parameters and the molecular field. The results give an idea about the predicted range of values of the constants K_i based on the values of $B_q^{(k)}$'s derived earlier for Fe^{2+} in YIG:Me^{4+} [10]. An attempt has been made to fit our theoretical K_1 and K_2 to the experimental values of K_1 and K_2 at low T for Fe^{2+} in YIG:Ge [18] obtained by neglecting the higher-order anisotropy terms. The calculations indicate that the experimental data [18] should be reconsidered taking into account the constants K_3 and K_4 in order to determine more reliably our model parameters $B_q^{(k)}$ and h from the experiment. The predicted temperature behaviour of K_1, K_2 and K_2/K_1 for Fe^{2+} in YIG:Ge speaks in favour of the present model rather than the doublet model previously employed. A test of applicability of the two models based on the predicted temperature behaviour of K_3 and K_4 is suggested. The experimentally observed change in sign of K_1 for Fe^{2+} in YIG:Si [17, 30, 31], which could not be explained by the doublet model with uniform distribution of Fe^{2+} ions, is now well understood in terms of our model. Similar fittings as for Fe^{2+} in YIG:Ge are performed for Fe^{2+} in YIG:Si resulting in a 'best' set of the values of $B_q^{(k)}$ and h.

The calculations of free energy as a function of temperature and the angle δ that magnetization makes with the axis [100] in the plane $(01\bar{1})$ have also been carried out. These results will be used in a subsequent paper to explain the recently observed spin reorientation in YIG:Si [6, 7] in terms of our model [19].

Acknowledgements

The author is very much in debt to Professor E. König for the hospitality during the author's stay at Erlangen. The Alexander von Humboldt Foundation research fellowship is also gratefully acknowledged. The author wishes to thank Professor S. Geller and Dr. P. Hansen for helpful correspondence. Thanks are also due to Dr. S. K. Kulshreshtha for several helpful comments and critical reading of the manuscript.

Appendix 1

The averages $\langle p^v q^v \rangle \equiv a + b\,\Phi + c\,Q$ of the angular quantities involved in the energies over the 12 inequivalent sites defined in Table 1. The average of $p\,q$, $p^3\,q$ and $p^5\,q$ equals zero.

Quantity	a	b	Quantity	a	b	c
q^2	1/3	0	$p^4 q^2$	1/27	0	−8/9
$p^2 q^2$	1/9	−2/9	$p^3 q^3$	$-1/(27\sqrt{2})$	$2/(9\sqrt{2})$	$-7/(9\sqrt{2})$
$p\,q^3$	$-1/(9\sqrt{2})$	$5/(9\sqrt{2})$	$p^2 q^4$	1/18	−1/6	2/3
q^4	1/6	1/6	$p\,q^5$	$-5/(54\sqrt{2})$	$5/(12\sqrt{2})$	$35/(36\sqrt{2})$
p^2	1/3	0	q^6	11/108	13/72	111/216
p^4	1/9	4/9	p^6	1/27	4/9	16/9

[1] G. Winkler, Magnetic Garnets, Vieweg, Braunschweig 1981.
[2] M. Wurlitzer and J. Franke, Phys. stat. sol. (a) **61,** K11 (1981); ibidem (a) **64,** 539 (1981).
[3] For relevant references prior to 1979 see Ref. [10] below.
[4] B. Antonini, S. Geller, A. Paoletti, P. Paroli, and A. Tucciarone, J. Mag. Mag. Mat. **22,** 203 (1981).
[5] F. Lucari, C. Mastrogiuseppe, E. Terrenzio, and G. Tomassetti, J. Mag. Mag. Mat. **20,** 84 (1980); F. Lucari, E. Terrenzio, and G. Tomassetti, J. Appl. Phys. **52,** 2301 (1981).
[6] S. Geller and G. Balestrino, Solid State Commun. **33,** 315 (1980).
[7] G. Balestrino, S. Geller, W. Tolksdorf, and P. Willich, Phys. Rev. **B 22,** 2282 (1980); Erratum, Phys. Rev. **B 23,** 3484 (1981).
[8] J. C. Slonczewski, J. Appl. Phys. **32,** 253 S (1961).
[9] C. Rudowicz, J. Appl. Phys. **50,** 7745 (1980).
[10] C. Rudowicz, Phys. Rev. **B 21,** 4967 (1980).
[11] R. Alben, E. M. Gyorgy, J. F. Dillon, Jr., and J. P. Remeika, Phys. Rev. **B 5,** 2560 (1972).
[12] C. Rudowicz, J. Phys. **C 14,** 923 (1981).

[13] M. I. Darby and E. D. Isaac, IEEE Trans. Magn. **10,** 259 (1974).
[14] P. Hansen, in Proceedings of the International School of Physics 'Enrico Fermi', Course LXX, Physics of Magnetic Garnets, Varenna, Italy, 1977; North Holland, Amsterdam 1978, p. 56.
[15] C. Rudowicz, J. Appl. Phys. **53,** 593 (1982).
[16] C. Rudowicz, J. Mag. Mag. Mat. (Jan. 1983), in press.
[17] A. Broese van Groenou, J. L. Page, and R. F. Pearson, J. Phys. Chem. Solids **28,** 1017 (1967).
[18] P. Hansen, W. Tolksdorf, and J. Schuldt, J. Appl. Phys. **43,** 4740 (1972).
[19] C. Rudowicz, J. Phys. Soc. Japan, submitted.
[20] C. Rudowicz and L. Kowalewski, Physica **80 B,** 517 (1975); C. Rudowicz, in Ref. [14] above, p. 467.
[21] J. C. Slonczewski, Phys. Rev. **110,** 1341 (1958).
[22] L. Kowalewski and C. Rudowicz, Magnetocrystalline Anisotropy of Ionic Oxide Compounds, Scientific Publications of A. Mickiewicz University, Poznań 1978 (in Polish); W. Döring, Ann. Phys. **1,** 102 (1958).
[23] R. Gonano, E. Hunt, and H. Meyer, Phys. Rev. **156,** 521 (1967); P. Röschmann and P. Hansen, J. Appl. Phys. **52,** 6257 (1981).
[24] T. S. Hartwick and J. Smit, J. Appl. Phys. **40,** 3995 (1969).
[25] M. D. Sturge, E. M. Gyorgy, R. C. Le Craw, and J. P. Remeika, Phys. Rev. **180,** 413 (1969).
[26] P. Hansen, Phys. Rev. **B 5,** 3737 (1972).
[27] J. Owen and J. H. M. Thornley, Rep. Prog. Phys. **29,** 675 (1966); D. Bloor and C. M. Copland, Rep. Prog. Phys. **35,** 1173 (1972).
[28] R. W. Teale, D. W. Temple, and D. I. Weatherley, J. Phys. **C 3,** 1376 (1970).
[29] C. Rudowicz, Acta Phys. Polon. **A 51,** 515 (1977).
[30] R. P. Hunt, J. Appl. Phys. **38,** 2826 (1967).
[31] J. H. Juddy, J. Appl. Phys. **37,** 1328 (1966).
[32] P. Paroli and S. Geller, J. Appl. Phys. **48,** 1364 (1977).